

HYPERSPECTRAL IMAGING OF PHOTOSYNTHESIS FROM THE SINGLE LEAF TO THE COMPLEX CANOPY - UNDERSTANDING THE SPATIO-TEMPORAL VARIATIONS OF PHOTOSYNTHESIS WITHIN A DROUGHT-STRESSED TROPICAL CANOPY

Uwe Rascher^{1, 2}, Caroline J. Nichol^{1, 3} and Chris Small⁴

1. Biosphere 2 Laboratory, Columbia University, Oracle, AZ 85623, USA
2. Institute of Chemistry and Dynamics of the Geosphere, ICG-III: Phytosphere, Forschungszentrum Jülich, Stettener Forst, 52425 Jülich, Germany; u.rascher@fz-juelich.de
3. School of GeoSciences, Darwin Building, Kings Buildings, University of Edinburgh, Mayfield Road, Edinburgh EH9 3JU, Scotland, UK; Caroline.Nichol@ed.ac.uk
4. Lamont Doherty Earth Observatory of Columbia University, Palisades, NY 10964, USA; small@ldeo.columbia.edu

ABSTRACT

Light use efficiency of photosynthesis adapts dynamically to environmental factors and is affected by internal and external stress factors, all of which lead to complex spatio-temporal variations of photosynthesis on various scales from the leaf to the canopy level. We tested a new, field portable hyperspectral imaging system (SOC-700), which produces 12-bit reflectance images between 440 and 880 nm with a 4nm spectral resolution. Data were filtered by smoothing the low order principal components reducing the noise of the instrument substantially. Leaf level scans of reflectance were used to detect differences in the non-photochemical energy dissipation of genetically modified *Arabidopsis thaliana* (L.) Heynh. mutants, which were deficient or over-expressed *psbS*, an intrinsic pigment-binding photosystem II subunit (also known as CP22). In a second experiment, the Photochemical Reflectance Index (PRI) was used to track drought stress induced inactivation of photosynthesis in leaves of four tropical tree species. Based on these leaf-level measurements a canopy element of the tropical rainforest in Biosphere 2 Centre was monitored using the same approach in the early morning after sunrise and two hours later when exposed to full sun. PRI developed a functional dependency only after activation of the biochemical non-photochemical energy dissipation processes were initiated after high light exposure. This study indicates the potential of hyperspectral reflectance measurements to quantify physiological adaptation of the photosynthetic apparatus and highlights the prerequisite to take structural and physiological heterogeneity of natural canopies into account.

INTRODUCTION

All life on Earth depends on the photosynthetic light capture and the use of this energy to convert CO₂ to carbohydrates. Stress factors such as nutrient limitations, availability of water, and extreme temperatures affect the efficiency of photosynthesis by influencing the function, biosynthesis, molecular assembly, and coordination of the components of the photosynthetic apparatus (i). These molecular mechanisms occur in the context of plant- and ecosystem-level responses to stress (ii). However, our knowledge of photosynthetic variability and exchange processes on the canopy or ecosystem level is still limited. Modelling studies that link global circulation models to atmospheric transport and physiological models have shown that ignoring stress responses may lead to erroneous conclusions (iii), emphasizing the need for more research concerning the effects of abiotic influences on plant ecosystem physiology.

The vegetation canopy is “the functional interface between 90% of Earth’s terrestrial biomass and the atmosphere” (iv), and terrestrial photosynthetic productivity is probably the most fundamental measure of global change of highest practical relevance to humankind. Net primary productivity

(NPP) of terrestrial ecosystems has been a subject of increasing interest because of the importance of terrestrial carbon cycle in global carbon budget. The spatial variation of net primary productivity (NPP) across the world in different ecosystems is enormous, ranging from 30 to 1000 g C m⁻² in different ecosystems (v). On the leaf level, the biochemical model proposed by Farquhar et al. (vi) and subsequently modified (vii, viii) is generally accepted and has been widely used to interpret and model leaf photosynthesis. The bottom-up scaling approach involved empiric species-dependent parameters and has proven effective in reproducing assimilation fluxes. The accuracy of the approach depends on the validity and robustness of the assumed scaling principles, which are strongly non-linear (ix). Additionally, natural ecosystems show distinct spatial heterogeneity in their response to stress factors, as recently shown at different tropical tree species during drought (x). Photosynthesis was differently affected by drought, with some trees having their photosynthetic efficiency reduced by 50%, while photosynthesis of other species under the same environmental conditions remained unaffected.

Even though global carbon models account for special heterogeneity in NPP and GPP (gross primary productivity), they rely on the accurate measurement of their input parameters, mainly light intensity (photosynthetic active radiation at 400-700nm; PAR), fraction of absorbed light (f_{APAR}) and a conversion factor, which describes the efficiency of conversion of absorbed light to carbon uptake (light use efficiency, LUE). While PAR and f_{APAR} can reliably be estimated from modelling and remote sensing data (xi), LUE cannot be measured on the ecosystem level and causes substantial uncertainties in global carbon models (xii). Additionally spatial and temporal heterogeneity of photosynthesis in canopies is a challenging feature of biological feedback between canopy processes, solar radiation and the atmosphere (xiii).

Remote sensing techniques and especially hyperspectral reflectance measurements have the potential to quantify photosynthetic efficiency of plants. Excess electrons in photosystem II are reduced via de-epoxidation of three pigments, violaxanthin, antheraxanthin, and zeaxanthin, while the accumulation of zeaxanthin serves as a quantitative indicator for non-photochemical energy dissipation (xiv, xv, xvi). The photosynthetic reflectance index (PRI) was developed to detect these bio-chemical changes and to serve as an estimate of photosynthetic light use efficiency (xvii, xviii, xix, xx). This normalized difference reflectance index, which uses two wavebands (531 and 570 nm) has been successfully used to detect changes in photosynthesis on the leaf level (xxi, xxii, xxiii, xxiv), small canopy level (xxv, xxvi, xxvii, xxviii) and recently at the ecosystem level (xxix, xxx, xxxi). Nevertheless, canopy and ecosystem measurements of PRI often have high uncertainty or failed to predict photosynthetic efficiency (xxxii).

Here we present a proof-of concept approach, that PRI and light intensity can be quantified with high spatial resolution from hyperspectral reflectance images in the field, detecting changes in light use efficiency occurring within hours on the leaf to canopy level.

METHODS

Plants

Leaf level measurements were performed using the wild-type, and the mutants L5 (PsbS protein over expressed), and npq4-1 (PsbS protein absent) of *Arabidopsis thaliana* (L.) Heynh. (ecotype Col-0). PsbS protein is essential for binding of the small subunit of the light harvesting complex to the photosystem core, and thus directly affects the non-photochemical energy dissipation via the xanthophyll cycle (xxxiii). *Arabidopsis thaliana* (L.) Heynh. plants were grown in a growth chamber at 100 $\mu\text{mol photons m}^{-2} \text{s}^{-1}$ and were exposed to full sun light (1300 $\mu\text{mol photons m}^{-2} \text{s}^{-1}$) for 25 minutes before measurements.

Leaves from four tropical trees, namely *Pterocarpus indicus* Willd., *Ceiba pentandra* L., *Pachira aquatica* Aubl. and *Inga cf. sapindoides* Willd., from inside the Biosphere 2 Center, Oracle, AZ, USA, were detached at the early morning and fixed on a cardboard under dim light (PFD < 1 $\mu\text{mol m}^{-2} \text{s}^{-1}$) using super-glue on the veins only (CN-polymer). The cardboard was then placed on the wall of an air-conditioned room at constant temperature and humidity (20°C and 60% RH). Leaves were dark adapted for 15 minutes after assembly, and then light (PFD = 160 - 190 $\mu\text{mol m}^{-2} \text{s}^{-1}$)

was provided by a 600 watts tungsten lamp (AL 1000, Arrilite, Germany). PFD was homogeneously distributed with a slight (15%) decrease towards the edges of the board. Leaves were subjected to drying under these constant conditions and measurements were taken after the onset of light and then after 1.5 and 6.5 hours. A calibrated reflectance panel (Spectralon, Labsphere, North Sutton, NH) was placed within the field of view to allow normalization of radiance values to reflectance.

Hyperspectral imaging of reflectance using the SOC-700

Hyperspectral images were acquired using the SOC-700 (Surface Optics, Corp., San Diego, CA, USA). Images have 640 x 640 pixels and a spectral resolution of ~4 nm with 120 equally distributed bands in the range of 410 - 910 nm (Fig. 1 and 2). The FWHM varies slightly with wavelength, but on average is 4.55 nm providing a minimum overlap of approximately 18%. The imager is a line-scanning push broom configuration. Light enters the instrument through the front aperture, travels through a pair of folding mirrors (one of which rotates to provide scanning) and enters the optical system through a C-mount lens, which can be adjusted (in our system: Schneider Xenoplan 1.9/35mm, resulting in a field of view of 0.015625 degrees per pixel). The lens images a column of data on to a horizontal slit at the entrance of the imaging spectrometer. The slit width (25 microns) determines the spectral resolution of the instrument as well as its light gathering capability. The imaging spectrometer is an ImSpector V9 (www.specim.fi) composed of the entrance slit, fore-optics, a prism-grating-prism spectrometer and some additional exit optics. The diffraction grating is of holographic design with an efficiency of approximately 50% over the entire spectral range. A 'row' of imaged points is spread out spectrally along the y-axis and then imaged on to a 640 x 480 pixel silicon CCD array, with a 12-bit dynamic range (PCO AG, Kelheim, Germany). The data are binned by 4 in the y-dimension to improve the signal to noise ratio resulting in a row of data, which is 640 pixels wide and 120 bands deep. Data are recorded for 640 scans and stored as 16 bit unsigned integer image cubes 640 x 640 x 120 pixels in extent. The first two dimensions are the spatial size of the image and the third dimension is the spectral. A single cube requires approximately 98 MB of storage space and can be processed and analyzed using the SOC software HS-Analysis or other hyperspectral processing packages such as RSI's ENVI software.

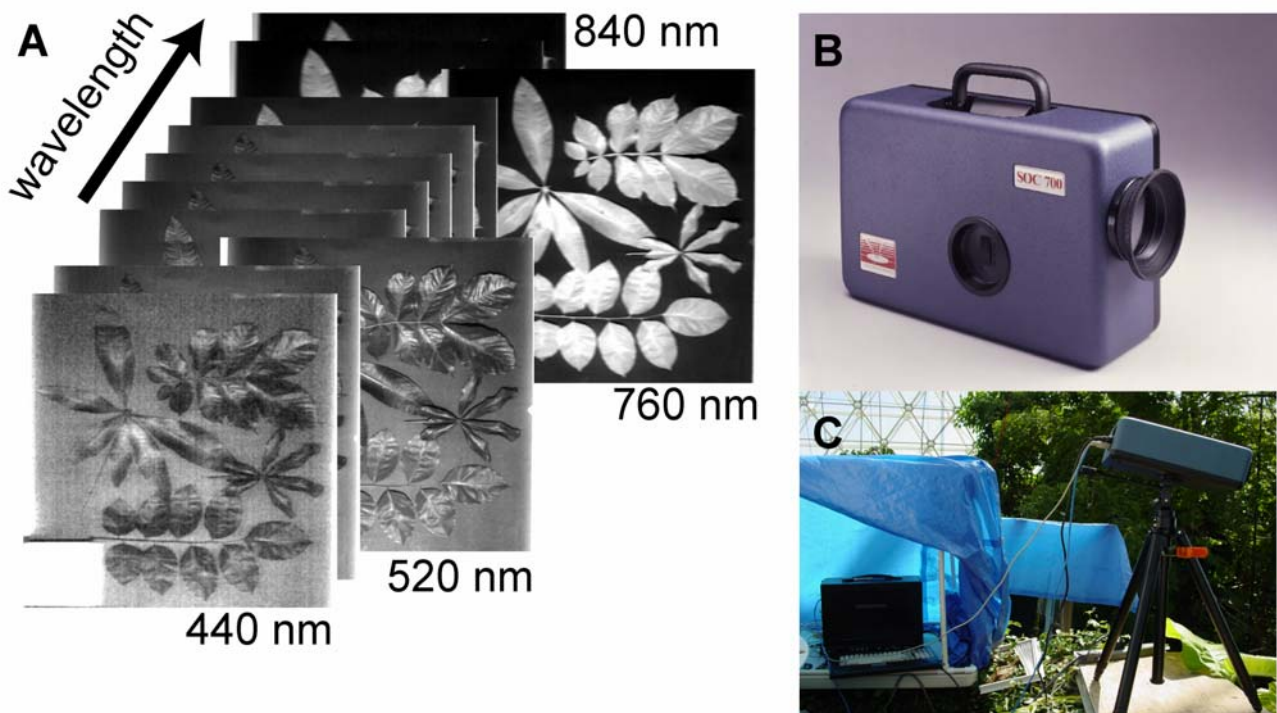


Figure 1: The SOC-700 hyperspectral imaging sensor. (A) Example of a hyperspectral cube of four tropical leaves (see further details below). (B) SOC-700 scanner (C) set-up of the SOC-700 in the tropical rainforest biome of Biosphere 2 Center. The control computer necessary for data acquisition is seen under the tarp.

The instrument yields absolute radiometric values as well as relative reflectance if a suitable standard is present for calibration or precise information is available regarding scene irradiance. SOC's HS-Analysis software compensates for the 700's spectral smile. Spectral smile is the slight deviation in wavelength as one reaches the edges of the spatial dimension and is characteristic of this type of imaging spectrometer. Dark noise compensation requires that prior to each measurement series a dark image be obtained to account for the inherent dark noise in the detector and electronics, which varies with exposure time and ambient temperature. Dark images are obtained by rotating the scan mirror until it is facing the spectrometer creating a dark path for imaging.

Data pre-processing

Hyperspectral cubes were linearly corrected using the dark image, acquired prior to each measurement, and normalized to a 50 calibrated reflectance standard (Spectralon, Labsphere, North Sutton, NH), which was provided in each image. All further analyses were performed using the reflectance images. Data at the extremes of the spectral range of the instrument appeared to be noisy, and thus, were not used in the analyses. Principal Component (PC) analysis suggests that the SOC-700 provides sufficient spectral redundancy to allow noise reduction by smoothing the high order PC. A Minimum Noise Fraction (MNF) transformation (xxxiv) was used to obtain the PC and estimate spectral dimensionality. Noise covariance statistics were derived from the corresponding dark image of the series. Spectral cubes were transformed to PC images, where each image was associated with an eigenvalue, which gives the variance associated with that PC image. PC vectors 1 - 3 contained most of the variance and were left unfiltered, as noise was negligible in these vectors. PC vectors of higher order showed greater noise levels; however, spatial information was clearly visible in images 4 - 12. In order to reduce the pixel to pixel variations, we convolved PC images 4 - 120 with a low-pass Gaussian kernel of 11 x 11. After filtering the high order PC images, the cubes were reconstructed using unfiltered PC vectors 1 - 3 and filtered PC vectors 4 - 120. Inverse MNF transformation yielded the original hyperspectral image cubes with a clearly reduced noise level and smoother spectra (Fig. 2A). For a further description see (xxiv).

Data analyses

The Normalized Differential Vegetation Index (NDVI) and Photochemical Reflectance Index (PRI, xvii) were calculated using pixel arithmetic according to eqs. 1 and 2, respectively:

$$NDVI = \frac{R_{780} - R_{670}}{R_{780} + R_{670}} \quad (1)$$

$$PRI = \frac{R_{531} - R_{570}}{R_{531} + R_{570}} \quad (2)$$

where $R_{\text{wavelength}}$ indicates the reflectance at this wavelength.

Single wavebands of the SOC-700 imaging system were approximately 4 nm apart; thus, wavelengths may not exactly meet the definition for PRI and may vary slightly with the single instrument calibration. We used the reflectance at the closest wavelength available, which in our case were 532.4 nm and 569.0 nm for the experiment with the detached tropical leaves and the canopy measurements and 530.5 nm and 571.6 nm for the measurements of *Arabidopsis thaliana* (L.) Heynh.

Signal to noise ratio (SNR) was computed according to eq. 3 using the spatially homogeneous spectralon reflectance panel.

$$SNR_{\text{wavelength}} = \frac{\overline{R}_{\text{wavelength}}}{\sigma_{\text{wavelength}}} \quad (3)$$

where $\overline{R}_{\text{wavelength}}$ is mean reflectance and $\sigma_{\text{wavelength}}$ is standard deviation at the wavelength.

Hyperspectral canopy measurements

Canopy images were acquired from a distance of about 10 meters. Images were taken at clear days inside the Biosphere 2 Center, Arizona, USA at 9:00 and 11:00 am from the canopy of *Pterocarpus indicus* Willd. Hyperspectral cubes were processed as described above (i.e. linearly corrected using the dark image, normalized to the reflectance standard, which was imaged just before each measurement, and filtered in Principal Component space). Images, which were captured at different times, were registered by manually selecting 10-20 control points and warping onto each other using polynomial functions and nearest neighbour re-sampling. The NDVI and PRI were calculated according to eqs. 1 and 2, respectively.

RESULTS

Hyperspectral image data

Radiance images from the SOC-700 were normalized using the reflectance standard provided in each image. The hyperspectral reflectance images of the leaves showed the characteristic spectra of living plant material (Fig. 2A). Raw-data were overlaid by noise, which could be greatly reduced by filtering of higher order Principal Components (Fig. 2A, see Material section and (xxiv) for a detailed description). Additionally, signal to noise ratio (SNR) in the infrared region increased due to the filtering process (Fig. 2B). SNR of all bands appeared to be comparable and all wavelengths were used for data analyses.

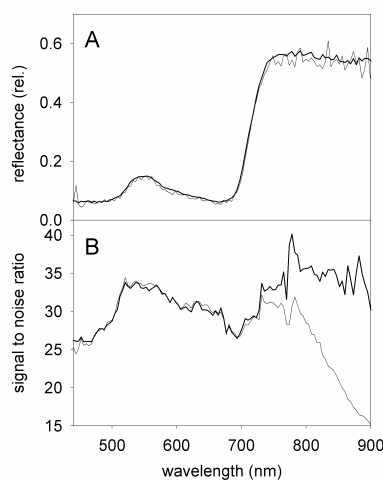


Figure 2: (A) Example of reflectance of a representative pixel of a *Pterocarpus indicus* Willd. leaf before filtering (thin line) and after filtering was applied (thick line). (B) Signal to noise ratio (SNR) of the SOC-700, calculated from the Spectralon reflectance standard (raw data: thin line; after filtering: thick line).

Spatial distribution of PRI in genetically modified plants

Light reaction of photosynthesis adapts to exposure to high light intensity and non-photochemical energy dissipation processes gradually increase within minutes and are known to saturate. Levels of saturation are increased for the L5 mutant and greatly decreased for the npq4-1 mutant (xxxv, xxxvi). PRI values of the three genetically different *Arabidopsis thaliana* (L.) Heynh. strains were different after 25 minutes of high light exposure (Fig. 3). npq4-1 mutants had the significant lowest (PRI = -0.071 ± 0.020 ; $P < 0.001$) and L5 mutants had the highest mean values (PRI = -0.052 ± 0.013). The wild-type plants had a slightly lower mean PRI than the L5 mutants (PRI = -0.054 ± 0.011), however, differences were not significant. Differences in PRI can be used to distinguish the three stains of *Arabidopsis thaliana* (L.) Heynh., which were undistinguishable for the bare eye (Fig. 3), which also highlights the potential of hyperspectral imaging for screening purposes in plant biotechnology.

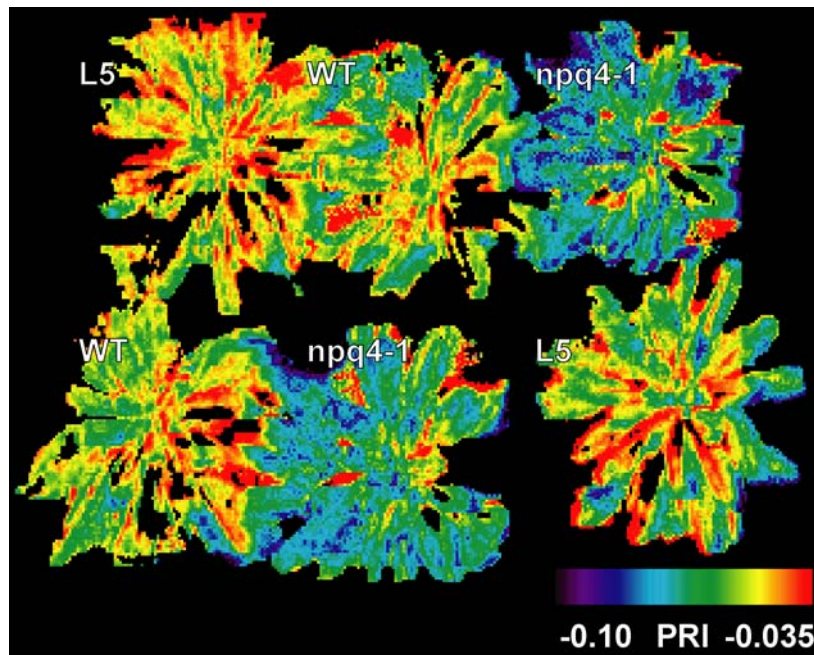


Figure 3: Map of Photochemical Reflectance Index (PRI) of three strains of *Arabidopsis thaliana* (L.) Heynh. after 25 minutes exposure to sun light ($PFD = 1300 \mu\text{mol m}^{-2} \text{s}^{-1}$). The three strains were wildtype (WT), over-expressed *PsbS* protein (L5) or were deficient of *PsbS* (*npq4-1*). A NDVI mask was used to display the leaf area only, colors code for different PRI values (see code at the lower right).

The effect of water stress on leaf-reflectance

Water stress generally affects both, leaf physiology and leaf structure. Structural changes are known to be primarily visible in the infrared region (xxxvii), while deactivation of photosynthesis should be reflected in the visible range and should be quantifiable using the PRI. Light reaction of photosynthesis of the four species was clearly affected by water stress as shown by chlorophyll fluorescence techniques (xxiv).

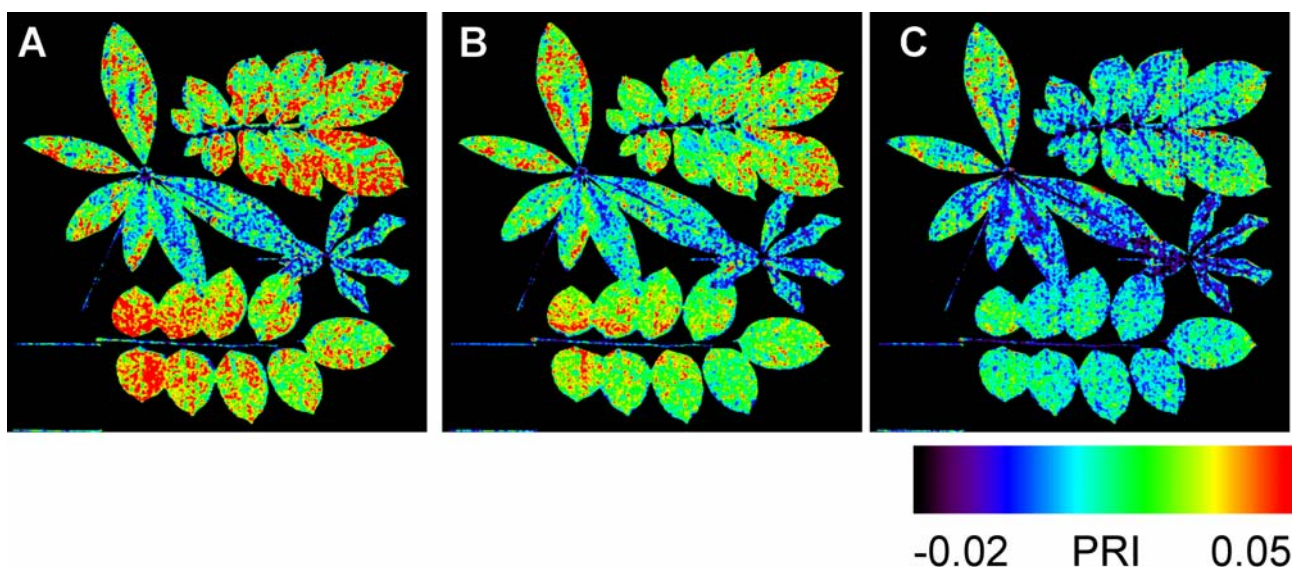


Figure 4: Time series of PRI during the drying process of four tropical leaves, which were exposed to light intensity of $150-180 \mu\text{mol m}^{-2} \text{s}^{-1}$ and which were exposed to water stress for 20 minutes (A), 1.5 hours (B) and 6.5 hours (C). A NDVI mask was used to display the leaf area only, colors code for different PRI values (see code at the lower right).

These changes in photosynthetic efficiency could be also detected in the PRI, which was monitored just after the exposure of light and then 1.5 and 6.5 hours after water stress (Fig. 4). PRI decreased with time of water stress, additionally showing pronounced heterogeneity over the single leaves. However, spatial heterogeneity, which was calculated for single leaves using cellular automaton techniques (xxxviii), did not change significantly during the drying process (personal communication M.T. Hütt). We assume that PRI is capable of tracking physiological changes in the photosynthetic apparatus, but it remains a noisy index, which is greatly affected by leaf structure, locally different surface structures, surface orientation of the leaf, and underlying noise of the instrument.

Spatial distribution of light and photosynthesis within the canopy

Intensity of the incident light was estimated and imaged from the green reflectance band at 550nm (R_{550nm}) of the hyperspectral cubes (Fig. 5 left row). Light was heterogeneously distributed within the canopy being reflected in the spatially patchy distribution of R_{550nm} . Photosynthetic efficiency is reflected in the PRI. Distribution of PRI, which shows high spatial variation at both measuring times, is shown in Fig. 5 right panel for the same canopy element of *Pterocarpus indicus* Willd.

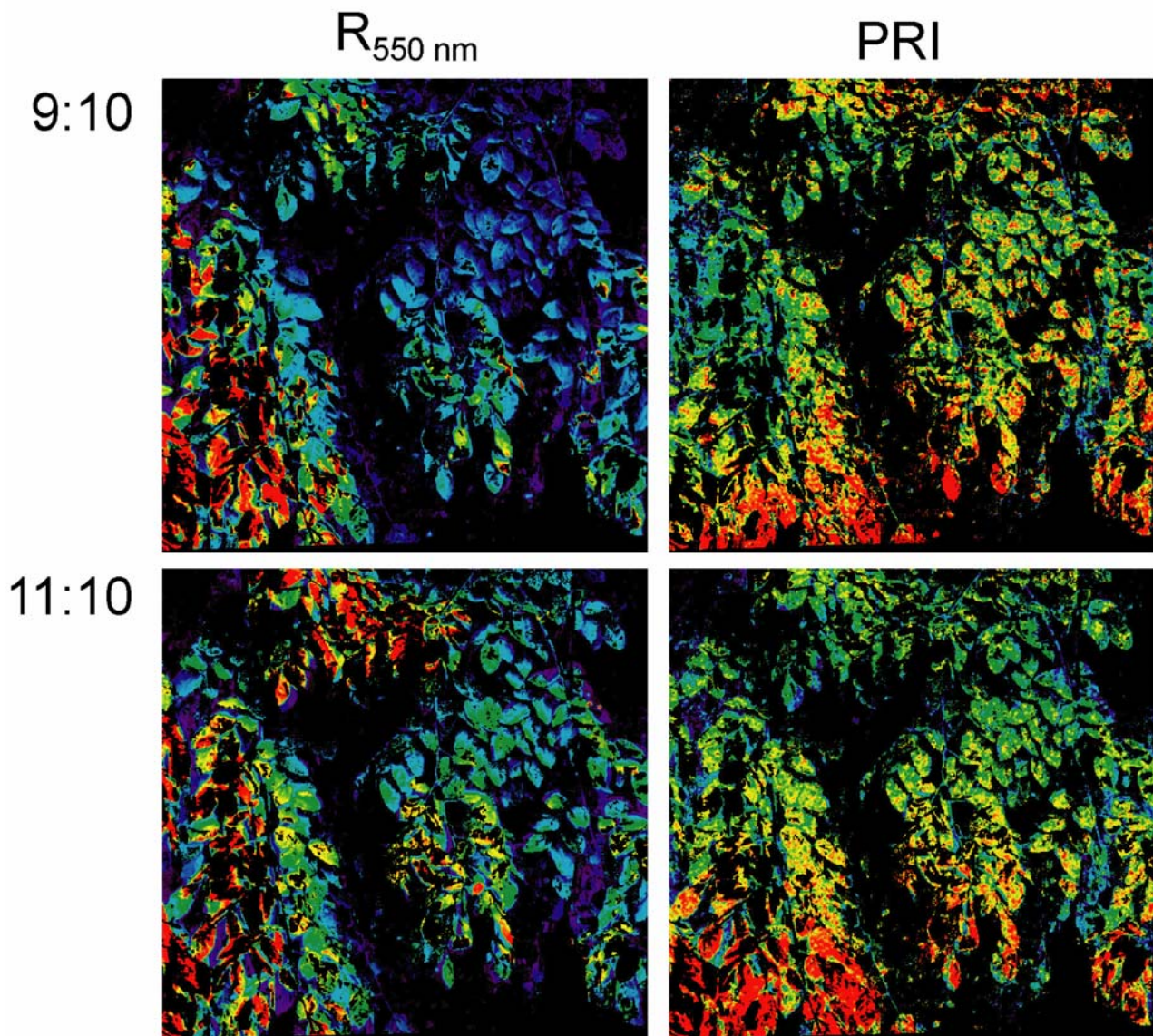


Figure 5: Maps of light intensity, quantified by the reflectance in the green (R_{550nm} ; left panels) and the Photochemical Reflectance Index (PRI; right panels). The same canopy element was monitored at the same day at 9:10 am and 11:10 am. Pictures are registered on each other. A NDVI mask was used to mask the pixels, which correspond to green leaf material only.

Correlation analysis of light and PRI distribution

We further investigated the dependency of PRI and light intensity and computed the correlation of R_{550nm} and PRI. No correlation was found between PRI and R_{550nm} at the 09:10 measurement. This relation changed within 2 hours and a non-linear dependency of PRI and R_{550nm} developed at 11:00. For low illuminated pixels PRI increased with R_{550nm} and then reached saturation at higher R_{550nm} values. As PRI correlates positively with photosynthetic efficiency, this dependency may well reflect typical light response characteristics of photosynthetic electron transport, which increases with increasing PFD and reaches saturation at higher PFD. Secondly, the dynamic development of this correlation during morning hours (9:00 until 11:00 am) points towards the biochemical adaptation of the photosynthetic apparatus and may reflect activation of the xanthophylls cycle, which constitutes a main element of non-photochemical energy dissipation (xiv, xvi). Nevertheless, we want to stress that these results and interpretation are preliminary and should serve as proof-of-concept data only. Nevertheless, spatial monitoring of PRI could provide inside in photosynthetic adaptation of canopy photosynthesis. Further data sets of additional species, which were monitored during the drought experiment, will be carefully tested for possible auto-correlation artefacts within the hyperspectral reflectance cubes.

CONCLUSIONS

The main driving factor determining light use efficiency of photosynthesis is light intensity which, if available in excess, can result in over-energetization of the photosynthetic apparatus, which induces biophysical and biochemical non-photosynthetic energy dissipation mechanisms (NPQ). One of the main biochemical NPQ processes includes the biochemical shift of the photosystem associated pigments violaxanthin and zeaxanthin (xanthophyll cycle). This biochemical shift can be detected in the reflectance signature of photosynthetic active tissue and the photochemical reflectance index (PRI) was found to detect changes in both, photosynthetic efficiency and NPQ on the leaf level. However, the xanthophyll cycle is only activated at high light conditions and has to be induced for some minutes. It is unclear how fluctuation light conditions as prevailing within natural canopies and during our measurements will affect the activation of the xanthophylls cycle. We assume that xanthophylls cycle was not activated in the early morning; and was imaged in its light activated state two hours later. These two physiological states may well be presented in the snapshots of PRI at 9:00 and 11:00 am, highlighting the potential of hyperspectral imaging to understand and scale the spatio-temporal dynamics of photosynthesis to the ecosystem level.

ACKNOWLEDGEMENTS

We greatly thank Xiao-Ping Li and Krishna Niyogi for providing the *Arabidopsis thaliana* (L.) Heynh. mutants. We thank Marc-Thorsten Hütt for the analyses of spatial heterogeneity. We also thank Surface Optics Inc., which provided the SOC-700 and made this survey possible. Financial support was provided by Mr. Edward Bass through a grant to Columbia University. This material is based upon work supported by the National Science Foundation under Grant No. 0340609.

References

- i Schulze E.D. & M.M. Caldwell, 1996. Ecophysiology of photosynthesis. Ecological Studies, vol. 100 (Springer, Berlin)
- ii Fitter A. & R.K.M. Hay, 2001. Environmental physiology of plants. 3rd edition (Academic Press) 367pp
- iii Sellers P.J., L. Bounoua, G.J. Collatz, D.A. Randall, D.A. Dazlich, S.O. Los, J.A. Berry, I. Fung, C.J. Tucker, C.B. Field & T.G. Jensen, 1996. Comparison of radiative and physiological effects of doubled atmospheric CO₂ on continental climate. Science, 271: 1402-1406
- iv Ozanne C.M.P., D. Anhof, S.L. Boulter, M. Keller, R.L. Kitching, F.C. Meinzer, A.W. Mitchell, T. Nakashizuka, P.L.S. Dias, S.J. Wright & M. Yoshimura, 2003. Biodiversity meets the atmosphere: a global view of forest canopies. Science, 301: 183-186
- v Scurlock J.M.O., W. Cramer, R.J. Olson, W.J. Parton & S.D. Prince, 1999. Terrestrial NPP: Toward a consistent data set for global model evaluation. Ecological Applications, 9: 913-919
- vi Farquhar G.D., S. von Caemmerer & J.A. Berry, 1980. A biochemical model of photosynthetic CO₂ assimilation in leaves of C₃ species. Planta, 149: 78-90
- vii von Caemmerer S. & G.D. Farquhar, 1981. Some relationship between the biochemistry of photosynthesis and the gas ex-change of leaves. Planta, 153: 376-387
- viii Sharkey T.D., 1985. Photosynthesis in intact leaves of C₃ plants: physics, physiology and rate limitations. Botanical Review, 51: 53-105
- ix Norman J.M., 1993. Scaling processed between leaves and canopy levels. In: Scaling Physio-logical Processes: Leaf to Globe, edited by J.R. Ehleringer & C.B. Field (Academic Press, San Diego), 41-76
- x Rascher U., E.G. Bobich, G.H. Lin, A. Walter, T. Morris, M. Naumann, C.J. Nichol, D. Pierce, K. Bil, V. Kudeyarov & J.A. Berry, 2004. Functional diversity of photosynthesis during drought in a model tropical rainforest – the contributions of leaf area, photosynthetic electron transport and stomatal conductance to reduction in net ecosystem carbon exchange. Plant, Cell & Environment, 27: 1239-1256
- xi Myneni R.B., R.R. Nemani & S.W. Running, 1997. Estimation of global leaf area index and absorbed PAR from radiative transfer models. IEEE Transactions on Geoscience and Remote Sensing, 35: 1380-1393
- xii Running S.W., P.E. Thornton, R. Nemani & J.M. Glassey, 2000. Global terrestrial gross and net primary productivity from the earth observing system. In: Methods in Ecosystem Science, edited by O.E. Sala, R.B. Jackson, H.A. Mooney & R.W. Howarth (Springer Verlag, New York), 44-57
- xiii Cox P.M., R.A. Betts, C.D. Jones, S.A. Spall & I.J. Totterdell, 2000. Acceleration of global warming due to carbon-cycle feed-backs in a coupled climate model. Nature, 408: 184-187

- xiv Demmig-Adams B. & W.W. Adams, 1992. Photoprotection and other responses of plants to high light stress. Annual Review of Plant Physiology and Plant Molecular Biology, 43: 599-626
- xv Demmig B., K. Winter, A. Krüger & F.C. Czygan, 1987. Photoinhibition and zeaxanthin formation in intact leaves: A possible role of the xanthophyll cycle in the dissipation of excess light energy. Plant Physiology, 84: 218-224
- xvi Horton P., A.V. Ruben & R.G. Walters, 1996. Regulation of light harvesting in green plants. Annual Reviews of Plant Physiology and Plant Molecular Biology, 47: 655-684
- xvii Gamon J.A., J. Peñuelas & C.B. Field, 1992. A narrow-waveband spectral index that tracks diurnal changes in photosynthetic efficiency. Remote Sensing of Environment, 41: 35-44
- xviii Gamon J.A., I. Filella & J. Peñuelas, 1993. The dynamic 531-nm Δ reflectance signal: a survey of 20 angiosperm species. In: Photosynthetic responses to the environment, edited by H.Y. Yamamoto & C.M. Smith (American Society of Plant Physiologists, Rockville, MD) 172-177
- xix Gamon J.A., L. Serrano & J.S. Surfus, 1997. The photochemical reflectance index: an optical indicator of photosynthetic radiation use efficiency across species, functional types and nutrient levels. Oecologia, 112: 492-501
- xx Peñuelas J., F. Baret & I. Filella, 1995. Semi-empirical indices to assess carotenoid/chlorophyll a ratio from leaf spectral reflectance. Photosynthetica, 31: 221-230
- xxi Peñuelas J., I. Filella & J.A. Gamon, 1995. Assessment of photosynthetic radiation-use efficiency with spectral reflectance. New Phytologist, 131: 291-296
- xxii Peñuelas J., J. Llusia, J. Pinol & I. Filella, 1997. Photochemical reflectance index and leaf radiation-use efficiency assessment in Mediterranean trees. International Journal of Remote Sensing, 13: 2863-2868
- xxiii Gamon J.A., L. Serrano & J.S. Surfus, 1997. The photochemical reflectance index: an optical indicator of photosynthetic radiation use efficiency across species, functional types and nutrient levels. Oecologia, 112: 492-501
- xxiv Rascher U., C.J. Nichol, C. Small & L. Hendricks. Monitoring spatio-temporal dynamics of photosynthesis with a portable hyperspectral imaging system. Photogrammetric Engineering & Remote Sensing, submitted.
- xxv Gamon J.A., J. Peñuelas & C.B. Field, 1992. A narrow-waveband spectral index that tracks diurnal changes in photosynthetic efficiency. Remote Sensing of Environment, 41: 35-44
- xxvi Filella I., J.L. Amaro, J.L. Araus & J. Peñuelas, 1996. Relationship between photosynthetic radiation use efficiency of barley canopies and the photochemical reflectance index (PRI). Physiologia Plantarum, 96: 211-216.

- xxvii Stylinski C.D., J.A. Gamon & W.C. Oechel, 2002. Seasonal patterns of reflectance indices, carotenoid pigments and photosynthesis of evergreen chaparral species. Oecologia, 131: 366-374
- xxviii Trotter G.M., D. Whitehead & E.J. Pinkney, 2002. The photochemical reflectance index as a measure of photosynthetic light use efficiency for plants with varying foliar nitrogen content. International Journal of Remote Sensing, 23: 1207-1212
- xxix Rahman A.F., J.A. Gamon, D.A. Fuentes & D. Prentiss, 2001. Modelling spatially distributed ecosystem flux of boreal forest using hyper-spectral indices from AVIRIS imagery. Journal of Geophysical Research, 106 (D24): 33579-33591
- xxx Nichol C.J., K.F. Hümmrich, T.A. Black, P.G. Jarvis, C.L. Walthall, J. Grace & F.G. Hall, 2000. Remote sensing of photosynthetic-light-use efficiency of boreal forest. Agricultural and Forest Meteorology, 101: 131-142
- xxxi Nichol C.J., J. Lloyd, O. Shibistova, A. Arneeth, C. Roser, A. Knohl, S. Matsubara & J. Grace, 2002. Remote sensing of photosynthetic light use efficiency of Siberian boreal forest. Tellus B, 54: 677-687
- xxxii Methy M., 2000. Analysis of photosynthetic activity at the leaf and canopy levels from reflectance measurements: a case study. Photosynthetica, 38: 505-512
- xxxiii Li X.P., P. Müller-Moulé, A.M. Gilmore & K.K. Niogi, 2002. PsbS-dependent enhancement of feedback de-excitation protects photosystem II from photoinhibition. Proceedings National Academy Science, 99: 15222-15222
- xxxiv Green A.A., M. Berman, P. Switzer & M.D. Craig, 1988. A transformation for ordering multispectral data in terms of image quality with implications for noise removal. IEEE Transactions on Geoscience and Remote Sensing, 26: 65-74
- xxxv Li X.P., O. Björkman, C. Shih, A.R. Grossman, M. Rosenquist, S. Jansson & K.A. Niyogi, 2000. Pigment-binding protein essential for regulation of photosynthetic light harvesting. Nature, 403: 391-395
- xxxvi Kolber Z.S., D. Klimov, G. Ananyev, U. Rascher, J.A. Berry & C.B. Osmond, 2005. Measuring photosynthetic parameters at a distance: laser induced fluorescence transient (LIFT) method for remote measurements of PSII in terrestrial vegetation. Photosynthesis Research, in press.
- xxxvii Carter G.A. & A.K. Knapp, 2001. Leaf optical properties in higher plants: linking spectral characteristics to stress and chlorophyll concentration. American Journal of Botany, 88: 677-684
- xxxviii Hütt, M.T. & R. Neff, 2001. Quantification of spatiotemporal phenomena by means of cellular automata techniques. Physica A, 289: 498-516